MISR JOURNAL OF AGRICULTURAL ENGINEERING
https://mjae.journals.ekb.eg/

ISSN-Print: 1687-384X
ISSN-Online: 2636-3062

Misr J. Ag. Eng., 39 (2): 281 – 298

DOI: 10.21608/mjae.2022.118501.1063

REDUCING THE THERMAL DEVIATION INSIDE GREENHOUSES BY USING SOLAR HEATING AND EARTH TUBE HEAT EXCHANGER SYSTEMS

Sameh Said Kishk[1]; Islam Hassan El-Sheikh[2] and Yahya Ejeez[3]

[1] Assoc. Prof., Ag. Eng. Dept., Fac. of Ag., Suez Canal U., 41522 Ismailia, Egypt.

[2] Prof., Ag. Eng. Dept., Fac. of Ag., Suez Canal U., 41522 Ismailia, Egypt.

[3] Demon., Ag. Eng. Dept., Fac. of Ag., Suez Canal U. 41522 Ismailia, Egypt.

* E-mail: s.kishk2011@yahoo.com

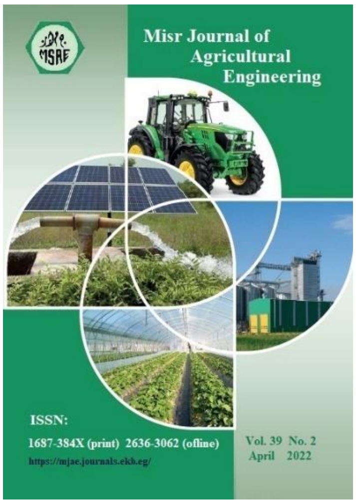

© **Misr J. Ag. Eng. (MJAE)**

Keywords:
Greenhouses; Earth-tube heat exchanger; Solar water heating; Solar tracking

ABSTRACT

Cucumber crops grow best between 18 and 25ºC of indoor air temperatures. When air temperatures fall below 16ºC or exceed 30ºC for extended periods, growth and yield are usually decreased. Therefore, the optimization of microclimatic conditions in greenhouses is particularly important in crop growth, development, and productivity. In this study, an attempt has been made to analyze the thermal performance of the solar heating system (SHS) and earth-tube heat exchanger (ETHE) during the winter season of 2020 (January to March). The experimental work was executed in the experimental farm of Faculty of Agriculture, Suez Canal University, Ismailia Governorate, Egypt (30.62ºN). Three identical gable-even-span polyethylene greenhouses each have a net floor surface area of 24 m^2. The first greenhouse (G1) was equipped with complete solar water heating. The second greenhouse (G2) was equipped with an earth-tube heat exchanger. While the third greenhouse (G3) was used as a control unit. The obtained data showed that the overall thermal efficiency of the earth-tube heat exchanger was 65%. The average overall thermal efficiency for solar water collectors was 59.6%. The average nightly indoor air temperatures for the three greenhouses (G1, G2, and G3) were 13.2, 11.6, and 9.3ºC, respectively. The total fresh yield of cucumber crop for the three greenhouses (G1, G2, and G3), respectively, 7.5, 6.3, and 3.8 kg/m^2.

1. INTRODUCTION

A greenhouse is a structure with walls and a roof made chiefly of transparent material, such as glass and plastic, in which plants requiring regulated climatic conditions are grown **(Imre, 2020).** Greenhouses are mainly designed, built, and operated to provide and maintain microclimatic conditions at the desired level for different crops. Greenhouse technology is a breakthrough in agriculture production technology that integrates market-driven quality parameters with production system profits (**Kumar *et al.*, 2009**).

Cultivation of crops in the greenhouse increases from high and low temperates regions. It is possible to produce these crops all year round in Egypt, even during the extremely cold winter season. Polyethylene greenhouses are used in Egypt on an increasingly large scale for the early production of warm-season vegetables, fruit, and flowers. It is a good application of solar energy collection for space heating and plant production. Moreover, its productivity per unit area is greater than the field production, and its product quality is always the highest (**Abed Elfattah *et al*.; 2014)**. The greenhouse technology also has tremendous scope in horticultural sector, especially for the production of hybrid seeds, high value vegetables, medicinal plants, cut flowers and fruits, which fetch more prices in domestic as well as international markets **(Yano *et al.*, 2019)**.
To achieve suitable growing conditions for vegetable crops inside the greenhouse, the inside air temperature must be controlled **(Vandecasteele *et al.*, 2020)**. Heating of greenhouse is one of the most energy consuming activities during winter periods. Although, it is an essential requirement for proper growth and development of winter growing crops **(Tiwari, 2003)**. Lack of heating has adverse effects on the yield, cultivation time, quality and quantity of the products in the greenhouse **(Ozgener and Hepbasli, 2007)**. Heating systems increase the capital and operational costs by 30 % and may be too expensive to use for most applications due to the high relative cost of energy systems. The use of low-cost and alternative heating systems is therefore of primary importance for a greenhouse to provide optimum indoor conditions during winter months **(Ghosal *et al.*, 2005)**.
It is well known that the temperature of the ground at a depth of about 2.5 to 3 m remains fairly constant around the year **(Bisoniya *et al.*, 2013)**. The earth-to-air heat exchanger system is considered an effective passive heating medium for different buildings. It mainly uses the stable temperature of the underground soil as a heat source and the air as the heat transfer medium for space heating during the winter season. The knowledge of soil thermal and physical properties (thermal conductivity, density, diffusivity, etc.), guides the designer in the selection of the type of earth to air heat exchangers (EAHE) system to be used and in the design of the system **(Milun *et al.*, 2005)**. EAHE consists of pipes buried in the soil, while an air circulation system forces the air through the pipes and eventually mixes it with the indoor air of the greenhouse **(Kishk, 2014)**. **Ghosal and Tiwari (2006)** developed a new thermal model for greenhouse heating and cooling with EAHE in New Delhi, India. The EAHE consisted of PVC pipes of 39 m in length. It was found on average 7-8°C higher than those of the same greenhouse without EAHE. **Shukla *et al.* (2006)** studied a thermal model for heating greenhouse by using different combinations of the inner thermal curtain, earth–air heat exchanger and geothermal heating. They found that earth–air heat exchanger provided an alternative source for greenhouse heating. **Tiwari *et al.* (2006)** studied the annual thermal performance of a greenhouse with an earth-air heat exchanger. They found that the temperature of the greenhouse increased by 4°C due to the use of an EAHE. **Nayak and Tiwari (2010)** carried out a theoretical performance assessment of an integrated photovoltaic and EAHE greenhouse**.** The results indicated that temperature inside the greenhouse can be increased by around 7-8°C during the winter season when the system operated with EAHE. **Zhao *et al*. (2019)** study the influence parameters on the thermal performance of the EAHE. They found the efficiency increases with increasing pipe length and decreases with increasing

pipe diameter. The hot water pipe heating system is mostly used for the large commercial greenhouse, and the location of the pipe near the ground is recommended to reduce the heat loss from the greenhouse.

Attar *et al.* (2014) evaluated the thermal performance of a greenhouse integrated with a solar heating system. The results indicated that the heating system could provide internal hot air with a temperature of about 6 ºC at night. **Hassanien *et al*. (2018)** evaluated the heating performance of a plastic- greenhouse (32 m^2) under the climate conditions of Kunming, China. Results indicated that the system can meet a significant portion of the total heat demand in October (62%), March (40%), and April (78%) at the desired heating temperature of 14ºC. **Kishk and Abu-Zeid (2019)** studied the experimental evaluation of two serpentine flat plate solar water heating systems. The experiments were carried out at different mass water flow rates of 0.45, 1.0, and 1.75 kg min^{-1}. The obtained results showed the thermal efficiency was 29.4, 39.3, and 48.5 % for flow rate 0.45, 1.0, and 1.7 kg min^{-1}, respectively. **Xu e*t al.* (2020)** proposed a water-circulating solar heat collection and release system with an indoor collector constructed of hollow polycarbonate sheets. The minimum nighttime air temperature heated by the system was increased by 3.9 °C during winter days. **Bazgaou *et al.* (2021)** studied the effect of active solar heating system on microclimate and fruit quality in greenhouse tomato production. They found that the solar heating system increased the total tomato yield by 55 % in winter period compared with the unheated system.

Numerous experiments have been performed upon the benefit of solar tracking system, revealing that up to 40% of additional energy can be attained by adopting the solar tracking method **(Banerjee, 2015).** According to **Khan *et al.* (2010)** a system that tracks the sun will be able to know the position of the sun in a manner that is not linear. The use of solar trackers can increase electricity production by around a third, and some claim by as much as 40% in some regions, compared with modules at a fixed angle **Guihua *et al.* (2012)** calculated the optical performance of horizontal single axis tracked solar panels. From the results the system increased the efficiency drastically around 36 %. **Watane and Dafde (2013)** studied the automatic solar tracking system. The designed that system which ensures 25 to 30% of more energy conversion than the existing static solar system. **Anusha *et al.* (2013)** compared the fixed and single axis solar tracking systems for 6 days. The results show that the solar tracking system increased the efficiency around 40%.

The main goal of the present study was investigating the greenhouses equipped with solar water heating and earth tube heat exchanger systems to warming greenhouses and maintain optimum growing environment for cucumber growth during winter season.

2. MATERIALS AND METHODS

The experimental work was carried out in the experimental farm of the Faculty of Agriculture, Suez Canal University, Ismailia, Egypt (Latitude angle of 30.62ºN and Longitude angle of 32.27ºE). It was executed during the winter season of 2020 (1st of January to 30th of March). Three identical gable-even-span form greenhouses were designed, constructed, and operated during this research work. The first greenhouse (G1) was equipped with a complete solar water heating system. The second greenhouse (G2) was equipped with an earth-tube heat exchanger system. In comparison, the third greenhouse (G3) was used as a control greenhouse trail. **Fig. (1)** shows the schematic diagram of the gable span greenhouse The geometric characteristics of the gable-even-span greenhouse are as follows: width 4.0 m and length 6.0 m, with a net surface area of 24 m^2, and volume 59.19 m^3. The rafters were tilted at 25^o to minimize the side effects of wind load on the greenhouse roof. The greenhouse structural frame was formed of 25.4 mm hot dipped galvanized pipes. The space between every three successive spans in a longitudinal direction is 4m. Greenhouses were orientated in the East-West direction and covered using a double layer of UV polyethylene sheets of 150 micron thick in order to reduce the heat energy loss from the greenhouse, particularly at nighttime.

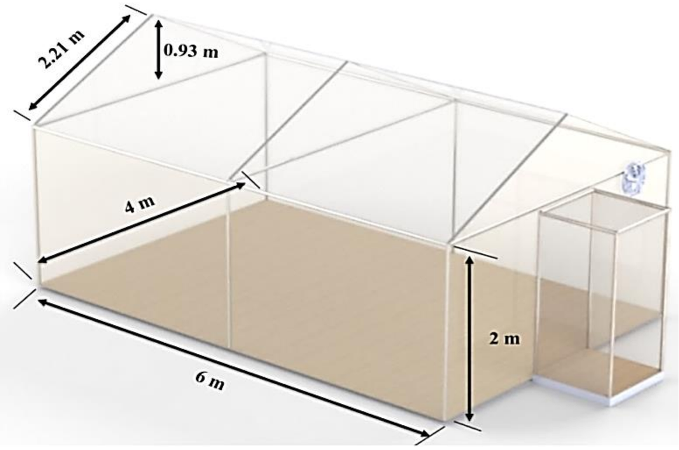

Fig. (1): Schematic diagram of the experimental greenhouse

Solar Heating System (SHS)

The tracked solar water heating system consists of five parts: solar tracking unit, solar collector panel, storage tank, water pump and heat exchanger, as shown in **Fig. (2).** A single axis tracker unit with one axis of rotation consists of light sensing devices, a control unit, and a driving mechanism. Light dependent resistor (LDR) as a light sensor has been used. The two light sensors are separated by a divider, which will create a shadow on one side of the light sensor if the solar panel is not perpendicular to the sun. For the controlling circuit, microcontroller ATMega328p acts as a brain that controls the movement of the motor via relay. Data received from the sensors and processed by the microcontroller. The tracker will be fixed when the light intensity received by both light sensors is equal. If light intensity received by one sensor was different from the other sensor, it means the sun moved to a new position and the whole collector should be rotated to face the sun in this new position. The signals from light sensors were transferred to a microcontroller unit to operate the DC motor of the driving mechanism for moving the solar water heater to this new position.

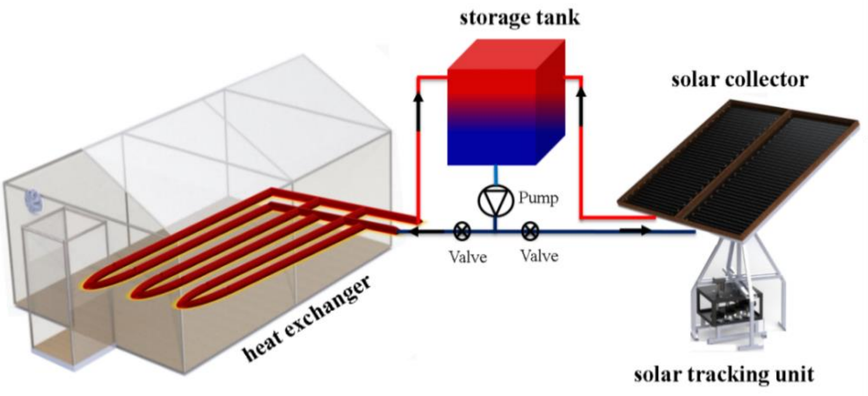

Fig. (2): Greenhouse with solar water heating

Fig (3) shows a flowchart of Arduino programming. The solar water heater consists of six components: a panel box, absorber plate, copper pipe, insulation material, glass cover, and water pump as shown in **Fig. (4).** The panel box was rectangular in shape and made from plywood with a thickness of 10 mm. The gross dimensions of the panel box were 2 m length, 1 m width, and 10 cm thickness, with a net upper surface of 1.5 m^2. The absorber plate is formed of an aluminum sheet which is a good conductor of heat and painted with matt black paint to absorb the maximum amount of solar radiation. The zigzag copper pipe (6 mm in diameter and 30 m length) was attached to the upper surface of the black absorber plate and painted by matt black. The gap between the wooden box and absorber plate was packed with 50 mm styrofoam (Thermal conductivity =0.04 W m^{-1} K^{-1}) to minimize heat losses. A clear glass cover with a 3 mm thickness was used to cover the solar panel box. Glass cover has been sealed with silicone rubber which plays an important role in promoting the efficient operation of the greenhouse effect as it accommodates the expansion and contraction between dissimilar materials. Collectors were positioned on a suitable steel structure and inclined at 31^o. Water was stored in a 0.5 m^3 cubic storage tank made from polyethylene and insulated by styrofoam layers. The stored hot water is pumped to the greenhouse air around the cucumber plants by the heat exchanger pipes. The heat exchanger was made from aluminum pipes (25.5 mm) and connected with a storage tank by fixable insulated polyethylene tubes. The system heat exchanger consists of six parallel rows of aluminum pipes. Finally, the water was continually cycled through the solar collectors and heat exchanger using a centrifugal pump with 375 watt, 30 L min^{-1} flow rate, and 20 m head.

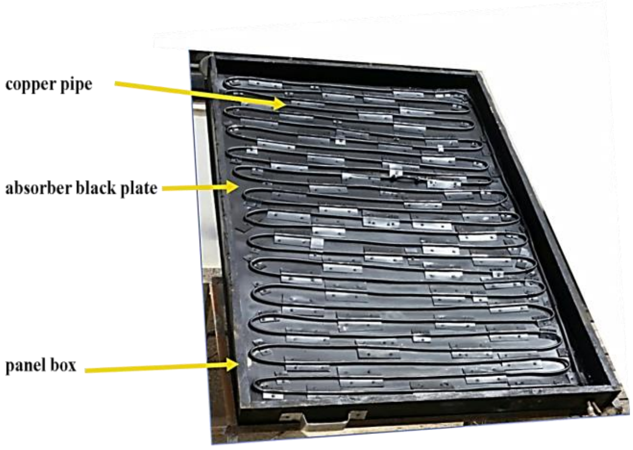

Fig. (4): Flat plate solar collector component

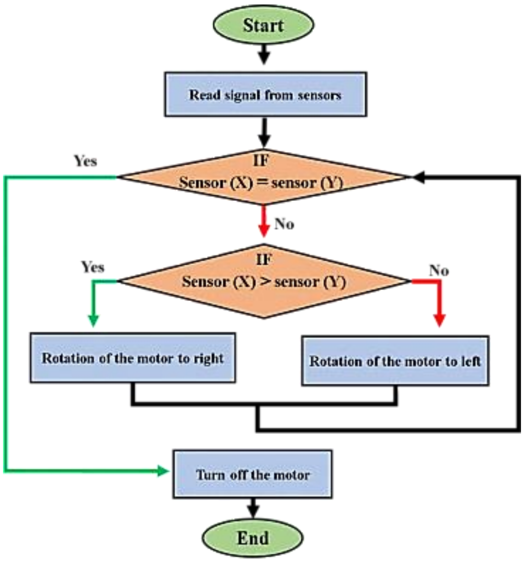

Fig. (3): Flowchart of arduino programming

Earth-Tube Heat Exchanger (ETHE)

The earth-tube heat exchanger was constructed and buried in the earth at a depth of 3 m. The earth-tube heat exchanger is 26 m long, 144 mm outer diameter, and made of 4 mm thick PVC tube as illustrated in **Fig. (5)**. The earth-tube heat exchanger system was operated as a single pass heat exchanger and the outlet airflow namely entered into the greenhouse one (G2). A portable blower (335 W power and flow rate of 1200 m^3 h^{-1}) has been fitted at the end of the earth-tube heat exchanger.

The earth-tube end was connected to the center of the eastern side of the greenhouse. A suction fan (1000 m^3 h^{-1}) was located on the above the end of the earth-tube heat exchanger. The suction fan was automatically operated (ON-OFF system) using a differential thermostat depending upon the indoor air temperature of the greenhouse. The outer opening area of the suction fan was covered with metal wire mesh to prevent entering the insects and foreign matters.

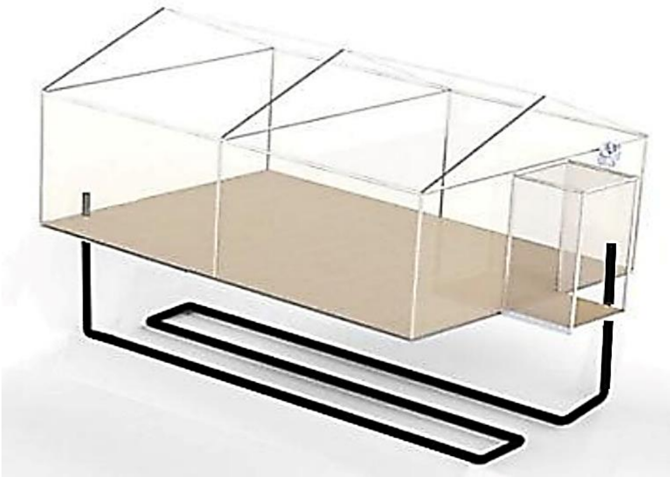

Fig. (5): Greenhouse with the earth-tube heat exchanger

Vegetating and Irrigation System

Cattle manure was added to the sandy soil during the preparation of root media inside the greenhouses by the rate of 15 m^3 per feddan. This rate was recommended for Cucurbitaceae family by **El-Shatoury (2005)**. The inside cultivable land of the three greenhouses was divided into three double piles, each pile having a gross dimension of 6 m long, 0.85 m wide, and 0.20 m high. Drip irrigation system was used inside the three greenhouses. It consisted of three components; main piping line, sub-main piping line (lateral line), and water pump in order to provide adequate hydrostatic pressure for maximum use rate of water**.** A galvanized water pipe (25.4 mm) was used as the mainline to pass the irrigation water from the water tank into the sub-main lines and the drippers. PVC pipe (19 mm) was used to pass the water uniformly throughout the drippers. Drippers (GR at 4 liter h^{-1} discharge) were uniformly alternative distributed with 35 cm dripper spacing throughout each row of plants. Five vegetative trays (84 growth blocks) were used to germinate the seeds of cucumber (Janco variety). Three hundred cucumber seedlings were selected at four real leaves instances and transplanted inside the three greenhouses.

Measurements and Data Acquisition Unit

Meteorological station (Vantage Pro 2, Davis, USA) located above the roof of the Agricultural Engineering Department, was used to measure different macroclimate variables such as, the solar radiation, dew-point, air temperatures, wind speed and its direction and air relative humidity**.** These sensors are connected to a data-logger system in order to test, display, and record the data during the experimental period. Data is displayed on the video screen and updated by scanning all the sensors. The means of 60 scans are recorded on hard disk every 5 minutes using software run to transfer the data automatically each day during the research work. Eight thermocouples were vertically located in the earth at different depths, starting at the soil surface and continuing at 1 m intervals to a depth of 3 m (two thermocouples for each point). The three greenhouses soil temperatures were measured at three different depths of 0, 0.1 and 0.2 m using six thermocouples in each greenhouse. The inlet and outlet temperature of the earth-tube heat exchanger were measured using four thermocouples. These sensors were connected to a data-logger system (Lab-Jack logger, powered by USB cable, supply 4-5.25 volt, USA) to display and record the data. Data is displayed on the video screen and updated by scanning all the sensors and stored in the computer files every 5 minutes. Another nine thermocouples were functioned to measure the indoor air temperatures inside the three greenhouses (three thermocouples for each greenhouse). Data included the measured indoor dry-bulb and wet-bulb temperatures were functioned to determine the indoor air relative humidity. The inlet and outlet water temperatures of the solar collector were measured using two thermocouples. Finally, the water temperature inside the storage tank was measured using one thermocouple. These sensors were connected to another data logger system (a 12 channels data logger digi - sense scanning thermometer) to display and record the data every 5 minutes.

Thermal efficiency of solar collectors

Thermal efficiency of solar water heating systems (η) is defined as the ratio of useful energy gain (Q_U) by the water to the solar radiation incident on the absorber of solar collector **Kurtbas and Turgut (2006)**

$$\eta = \frac{Q_U}{I.\,A} \qquad (1)$$

It is also known that the heat absorbed by the water (useful heat) is determined by the relationship **(Kishk and Abu-Zeid, 2019)**:

$$Q_u = m c_p \left(T_o - T_i\right) \qquad (2)$$

Energy stored (QS) by heating system (**Kishk and Abu-Zeid, 2019)**:

$$Q_S = M c_p \left(T_a - T_b\right) \qquad (3)$$

Where:

A solar collector area, m^2

C_p specific heat of water, 4186 J kg^{-1} K^{-1}

I intensity of solar radiation, Wm^{-2}

M mass of water in storage tank, kg

T_i, T_o inlet and outlet collector water temperature, respectively, K

T_a, T_b storage tank temperature at the end and the beginning of each day, respectively, K

Effectiveness of earth-tube heat exchanger (ETHE)

The effectiveness of the earth-tube heat exchanger for heating mode (η_h) was computed using the following two equations **(Al-Ajmi *et al*., 2006)**:

$$\eta_h = \frac{T_o - T_i}{T_s - T_i} x100 \qquad (4)$$

The potential heating acquired from the earth-tube heat exchanger (Q_{exc}) can be calculated using the following equation **(Li *et al*., 2014)**:

$$Q_{exc} = \dot{m}\ C_{pa}\ (T_o - T_i) \qquad (5)$$

Where:

η_h = effectiveness of earth tube heat exchanger, %

T_i and T_o = inlet air temperature of earth-tube heat exchanger, K

T_s = sandy soil temperature at depth 3.0 m, K

Q_{exc} = heat exchange rate, kW h day^{-1}

$\dot{m}$ = mass flow rate of air, kg s^{-1}

C_{pa} = specific heat of air, J kg^{-1} K^{-1}

3. RESULTS AND DISCUSSION

Average monthly macroclimatic conditions throughout the experimental periods from the 1st of January till 30th of March, 2020 were measured, summarized, and listed in **Table (1)**. During the winter season, the average monthly ambient air temperatures and air relative humidity were 15.7 ºCand 61.8 %, While the average monthly solar radiation flux incident on the horizontal plane was 367.0 W m^{-2}. Finally, the average monthly wind speed, blowing over the greenhouses cover during the same periods was 1.5 m s^{-1}.

Table (1): Average monthly macroclimatic conditions through out the experimental periods

Month	Ambient air temperature, ºC	Humidity, %	Wind speed ms^{-1}	solar radiation W m^{-2}
January	14.3	64.9	1.2	302.9
February	15.7	60.1	1.3	404.7
March	17.0	57.4	1.8	434.0
Mean	**15.7**	**61.8**	**1.5**	**367.0**

Solar Water Heating System

The hourly variation of the solar radiation intensity, ambient air temperature, inlet and outlet water temperatures for the solar collector during winter months are shown in **Fig. (6).** It can clearly be seen that the solar radiation intensity and ambient air temperature gradually increased from sunrise until reaching the maximum value at noon, and then it gradually decreased until reaching the minimum value prior to sunset. The outlet water temperature depends on some parameters such as the intensity of the incident solar radiation, ambient air temperature, and mass flow rate. From **Fig. (6),** it is found that the average outlet water temperature increases with the increase of solar radiation. The illustration shows that the highest outlet water temperature was obtained between 13:00 pm and 14:00 h under the maximum solar radiation incident. It is noticed that the average inlet and outlet water temperatures for January month were found to be 38.5 and 44.3ºC. Also, the average inlet and outlet water temperature for February were found to be 41.7 and 49.1ºC. Meanwhile, the average inlet and outlet water temperatures for March month were found to be 43.3 and 51.3ºC.

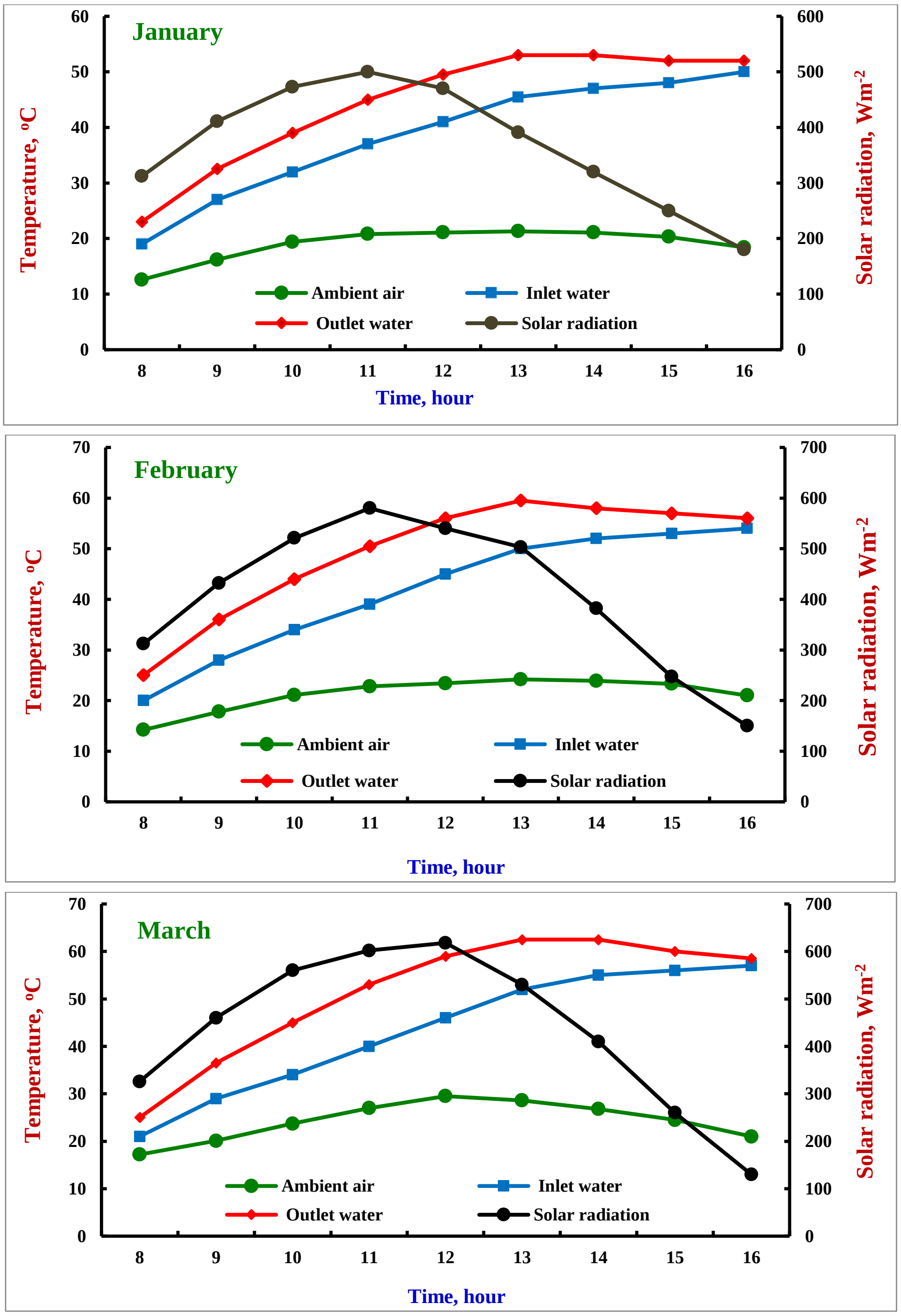

Fig. (6): Average ambient air temperature, inlet, outlet water collector temperature and solar radiation during winter months of 2020

Fig. (7) depicts the temperature difference between the inlet water, outlet water collector and thermal efficiency during the winter months. It is obvious that the temperature differences increased in the morning hours and attain maximum values at local solar noon and decreased in the evening hours. It is noticed that the water temperature difference ranged from (2 to 8.5 ºC), (1.1 to 11.5 ºC) and (1.5 to 13ºC) with average 5.8, 7.2 and 8.0 ºC for January, February, and March months, respectively. The temperature difference between inlet and outlet water collector is higher for higher solar radiation. These data are in agreement with that published by **Bolaji (2006)**. The most important part of this study was evaluating the thermal efficiency of the solar collector. **Fig. (7)** shows the variations of thermal efficiency curves of the solar water collector under the average prevailing weather conditions. The thermal efficiency was low in the morning and afternoon because the solar intensity was low at that time. However, in the noon, the thermal efficiency was high because the temperature differences between the inlet and outlet of the water were high. For the duration of the experimental tests, the monthly average thermal efficiency was 56.1, 60.3, and 62.3 % for the January, February, and March months, respectively, which gave an average overall thermal efficiency of 59.6 %.

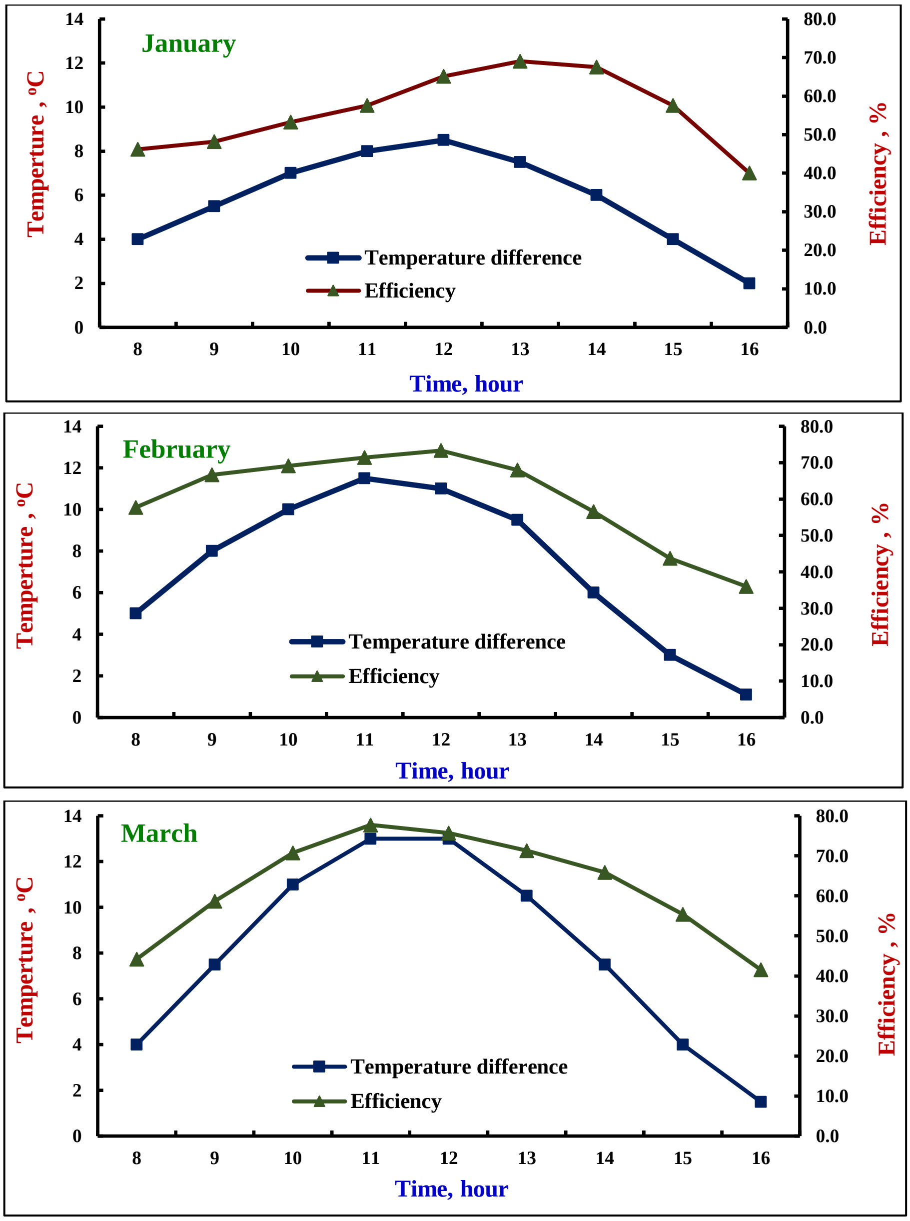

Fig. (7): Average temperature difference between inlet and outlet water and solar collector efficiency during winter months of 2020

Fig. (8) shows the variation of stored energy in the storage tank produced from the collector. The average stored energy during January, February, and March months was 51.91, 56.93, and 60.28 MJ, respectively. The highest stored energy occurred during March month. Due to the stored energy depends on the total solar radiation and ambient air temperature.

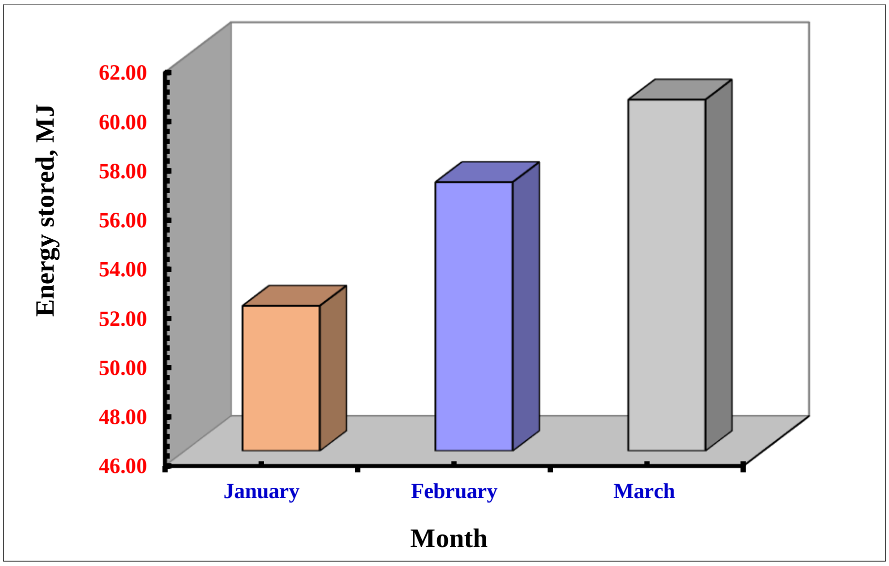

Fig. (8): Stored energy inside storage tank asfunction of time

Earth-Tube Heat Exchanger System

Fig. (9) reveals the relationship between the average monthly minimum ambient air temperature, peripheral deep soil temperature at 3 m depth and optimum night temperature. This figure evidently indicates that the 3 m deep soil temperature was continuously higher than the optimum night temperature (18°C) throughout the winter months. It also shows a great difference between the optimum night temperature and minimum ambient air temperature during winter months. This difference was on average 7.5°C, whilst the potential difference between the average deep soil temperature at 3m depth and optimum night temperature was 3.8°C.

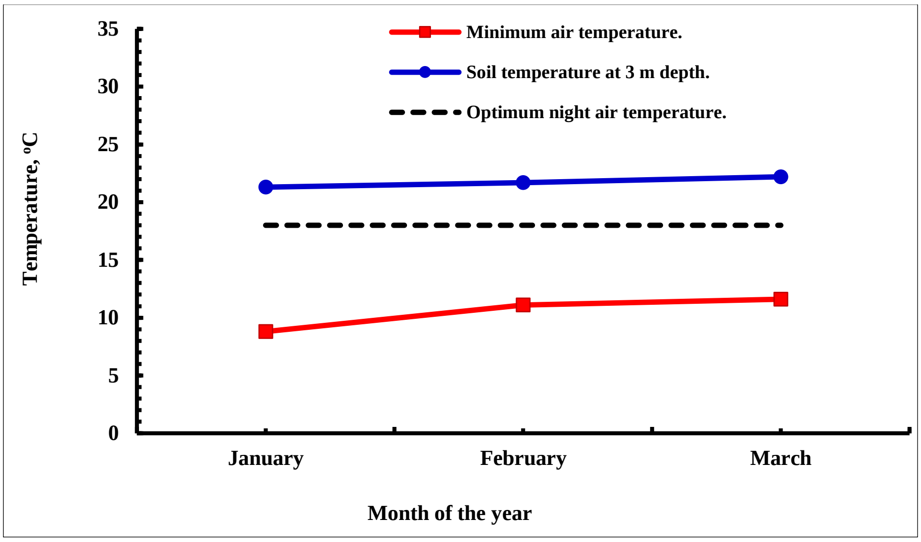

Fig (9): Average monthly minimum ambient air temperature, peripheral deep soil temperature at 3 m depth and optimum night air temperature

It is imperative to determine the effectiveness of earth-tube heat exchanger which was functioned to heat the indoor air of the greenhouse in order to realistically evaluate the possibility of using that system as an alternative source of energy. The average monthly inlet airflow temperature, outlet airflow temperature, peripheral deep soil temperature at 3 m deep, and thermal efficiency of the earth-tube heat exchanger throughout the winter season of 2020 are summarized and listed in **Table (2).** It obviously indicates that the thermal efficiency of earth-tube heat exchanger system was continuously variable depending upon the temperature difference between outlet and inlet earth-tube airflow and temperature difference between peripheral deep soil temperature and inlet earth-tube airflow. It also reveals that the lowest inlet airflow temperature was on average 12.3ºC and occurred in January. During this month, the greatest average temperature increase (6.5ºC) for the earth-tube airflow and, consequently, the greatest average thermal efficiency of the earth-tube heat exchanger (72.2 %) was achieved. Whereas the greatest inlet earth-tube airflow temperature was on average 16.0ºC and occurred in March. For the duration of this month, the lowest average temperature increase (3.7ºC) for the earth-tube airflow and, consequently, the lowest average thermal efficiency (59.7 %) of the earth-tube heat exchanger were performed. The table also shows that the monthly average daily overall thermal efficiency values for January, February, and March months, were 72.2%, 61.7 %, and 59.7 %, respectively, which gave an average overall thermal efficiency of 65.0%. The low ambient air temperature for the three winter months (from January to March) ranged from 8.8 to 11.6ºC. These low ambient air temperature conditions were provided a high heat exchange rate for the specific earth-tube heat exchanger system and surrounding thermal mass of the deep soil. The monthly average daily energy heat exchange rate and temperature patterns are summarized and listed in **Table (2)**. It evidently shows that the greatest value of heat energy exchange rate (2.52 kWh) occurred in January, when the monthly average daily inlet airflow temperature was quite low (12.3ºC). Whereas the lowest magnitude of heat energy exchange rate (1.51 kWh) was achieved in March month with an inlet airflow temperature of 16.0ºC. It also reveals that the seasonal average daily heat energy exchange rate throughout the heating mode was 1.95 kWh.

Table (2): Average monthly inlet airflow temperature (T_{ai}), outlet airflow (T_{ao}), soil temperature at 3 m deep (T_s), overall thermal efficiency (η_h) and energy exchange rate (Q_{exc})

Month	T_{ai} , ºC	T_{ao} , ºC	T_s , ºC	η_h, %	Q_{exc} , kWh/day
January	12.3	18.8	21.3	72.2	2.52
February	15.7	19.4	21.7	61.7	1.83
March	16.0	19.7	22.2	59.7	1.51
Mean	**14.7**	**19.3**	**21.8**	**65.0**	**1.95**

The seasonal average hourly heat energy exchange rate of the earth-tube heat exchanger system, which is related to the inlet and outlet airflow temperatures for the winter season, is demonstrated together in **Fig. (10)**. This figure shows an inverse relationship between the heat energy exchange rate and the inlet airflow temperature. It obviously shows that the hourly maximum heat energy exchange rates were normally provided at the end of nighttime when the lowest ambient air temperatures occurred. It also reveals that the minimum heat energy exchange rates were normally recognized at the first hour of starting when the warmest ambient air temperatures were provided.

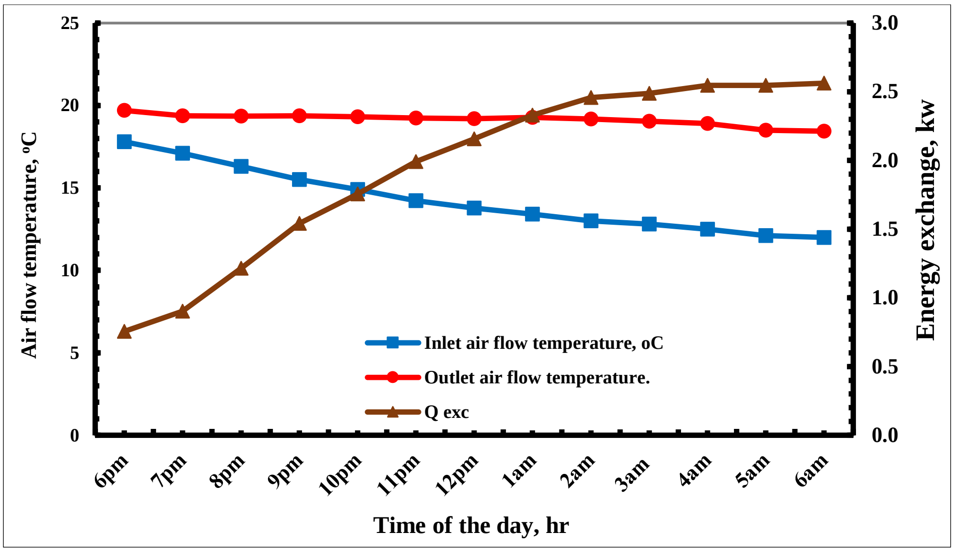

Fig. (10): Seasonal average heat energy exchange rate related to the inlet and outlet airflow temperatures

Air temperature and relative humidity

For the duration of the heating period (from January to March 2020), the seasonal average hourly outdoor and indoor air temperatures for the three greenhouses (G1, G2 and G3) are plotted in **Fig. (11).** The hourly average outdoor and indoor air temperatures for the three greenhouses (G1, G2 and G3) were 13.6, 18.4, 17.5 and 16.0ºC, respectively. Also, the average nightly indoor air temperatures for the three greenhouses (G1, G2 and G3) and outdoor air temperatures during the heating period were 13.2, 11.6, 9.3, and 9.4ºC, respectively. It also reveals that the nightly average indoor air temperature of the greenhouse (G1 and G2) was higher than that of the control greenhouse (G3) by 3.3 and 1.7ºC (36.3 and 17.2 %). Finally, the nightly average indoor air temperature of greenhouses (G1) and (G2) were continuously at and around the optimal level (18ºC) due to the incoming warm air from the earth-tube heat exchanger system and heat extract from the solar water system. While the nightly average indoor air temperature of the control greenhouse (G3) was continuously lower than the optimum air temperature.

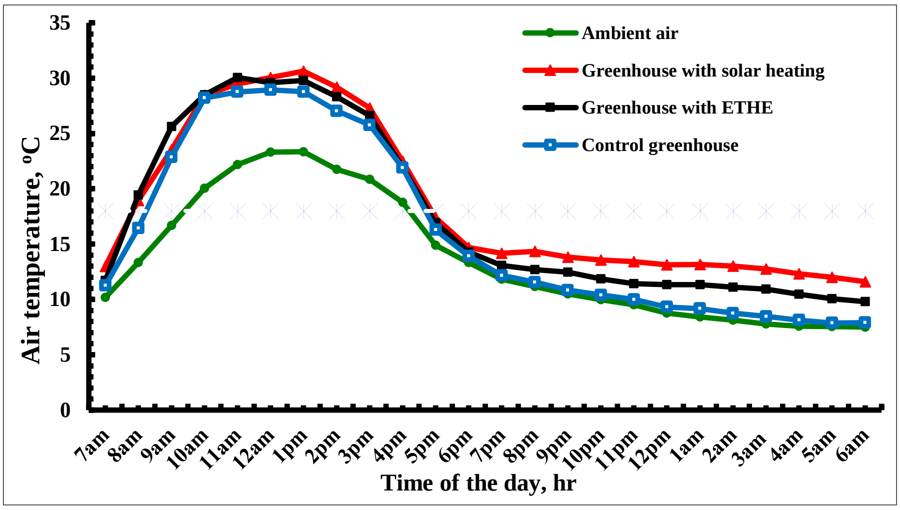

Fig. (11): Changes in indoor and outdoor air temperatures for the three greenhouses as a function of time during the heating period

The air relative humidity inside the three greenhouses, respectively, ranged from 48.0 to 74 %, 47 to 71 and 44 to 87 %, whereas the outside air relative humidity was in the range of 45.5 to 81.4 %. Consequently, solar heating and the earth-tube heat exchanger system reduced the indoor air relative humidity compared with the control greenhouse. Air stream passed through the longitudinal direction of the greenhouse (G2), which comes from the earth-tube heat exchanger system,alleviating the side effects of excessive air relative humidity by moving warm air across plant surfaces to keep them dry. The warm air stream passing through the greenhouses (G1 and G2) led to prevent the temperature stratification and related pests and prevent condensation occurrence. Normal plant growth inside the greenhouse generally occurs at air relative humidity ranging from 50 to 80 % **(Hanan *et al.*, 2003)**. Low indoor air temperature and high indoor air relative humidity increase the possibilities of infection by pathogenic organisms.

Cucumber Plants

The cucumber plants were transplanted at the same time inside the three greenhouses at 4 true leaves with an average length of 6 cm. The weekly averages increasing rate in number of cucumber leaves inside the three greenhouses (G1, G2 and G3), respectively were 2.45, 2.21 and 1.85 leaf/plant. As the number of leaves is increased, the green surface area of the plant is increased. This agrees with the data published by **Nelson (2006).** The maximum lengths of the cucumber plants inside the three greenhouses were 143.1, 125.2 and 85.6 cm, respectively as shown in **Fig. (12)**. The averages stem length of cucumber plants for the three greenhouses (G1, G2 and G3) were 70.2, 60.3 and 45.9 cm, respectively. Thus, the greenhouses (G1, and G2) increased the stem length over the control greenhouse (G3) by an average 52.9 and 31.3 %. Fresh yield of cucumber crop for the two greenhouses (G1, G2 and G3), respectively, was 7.5, 6.3 and 3.8 kg/m^2 as revealed in **Fig. (13)**. Therefore, the greenhouses (G1 and G2) were found to be 3.7 and 2.5 kg/m^2 (97.3 and 65.7 %) more productive than that the greenhouse (G3). These obtained data confirmed the finding by **(Ghosal and Tiwari, 2006)** when they stated that, under ventilating and heating conditions of greenhouses, more rapid growth and greater fresh yield were achieved than that grown without heating the indoor air.

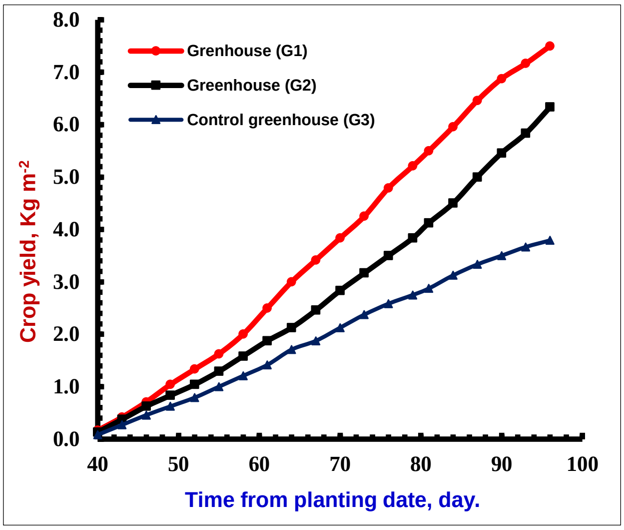

Fig. (12): Stem length of cucumber plants for the three greenhouses (G1, G2 and G3)

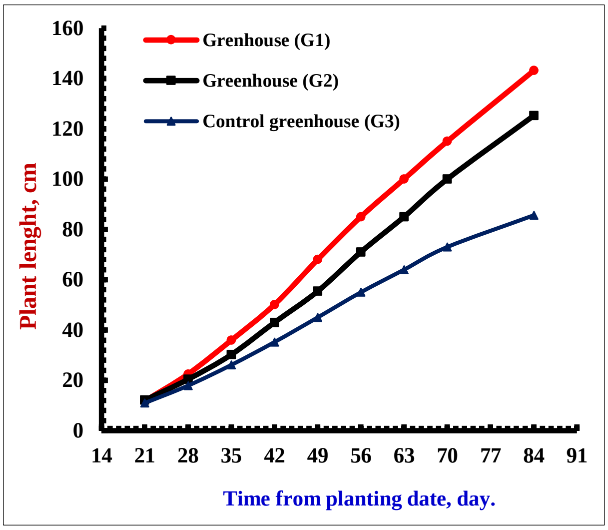

Fig. (13): Fresh yield of cucumber crop for the three greenhouses (G1, G2 and G3)

4. CONCLUSION

- The average overall thermal efficiency of the earth-tube heat exchanger system was 65% for the whole heating mode. The average overall thermal efficiency for the solar water collector was 59.6 %. The average stored energy during January, February and March months was 51.91, 56.93 and 60.28 MJ, respectively.
- The seasonal average nightly indoor air temperatures for the three greenhouses (G1, G2 and G3) and outdoor air temperatures during the heating period were 13.2, 11.6, 9.3, and 9.4ºC, respectively. It also reveals that the nightly average indoor air temperature of the greenhouse (G1 and G2) was higher than that of the control greenhouse (G3) by 3.3 and 1.7ºC (36.3 and 17.2%).
- The maximum lengths of the cucumber plants inside the three greenhouses, respectively, were 143.1, 125.2 and 85.6 cm. Thus, the greenhouses (G1, and G2) increased the stem length over the control greenhouse (G3) by an average 48.1 and 32.6 %. The total fresh yield of cucumber crop for the three greenhouses (G1, G2 and G3), respectively, was 151, 131 and 91 kg/m^2. The greenhouses (G1 and G2) were found to be 3.7 and 2.5 kg/m^2 (97.3 and 65.7 %) more productive than the greenhouse (G3).

5. REFERENCES

Abed Elfattah, S.; Mostafa, M. M.;Elnono, M. A.and Kassem, A. M. (2014) "Greenhouse heating and ventilation control system" Misr J. Ag. Eng., 31 (2): 667 - 682

Al-Ajmi, F.; Loveday, D. L. and Hanby, V. I. (2006) "The cooling potential of earth-air heat exchangers for domestic buildings in a desert climate" Building and Environment, 41, 235-244.

Anusha, K.; Chandra, S. and Mohan, R. (2013) " Design and development of real time clock based efficient solar tracking system" International journal of Engineering Research and Applications (IJERA) 3, 1219-1223.

Arnold, K. A.; Camplell, G. S.; Nielsen, D. R.; Jackson, R. D.; Chair, A. K. and Morthand M. M. (1986) "Methods of soil analysis" Part (1) Physical and Mineralogical Methods second edition, American Society of Agronomy, Inc. Ch (15): 383-409.

Attar, I. ; Naili, N. ; Khalifa, N. ; Hazami, M. ; Lazaar, M. and Farhat, A., (2014) "Experimental study of an air conditioning system to control a greenhouse microclimate" Energy Convers. Manag. 79, 543-553.

Banerjee, R. (2015) "Solar Tracking System". International Journal of Scientific and Research Publications, 5 (3) 2250-3153.

Bazgaou, A.; Fatnassi, H.; Bouharroud, R.; Ezzaeri, K.; Gourdo, L.; Wifaya, A. and Bouirden, L. (2021) " Effect of active solar heating system on microclimate, development, yield and fruit quality in greenhouse tomato production" Renewable Energy, 165, 237-250.

Bisoniya, T. S.; Kumar, A. and Baredar, P. (2013) "Experimental and analytical studies of earth–air heat exchanger (EAHE) systems in India: A review" Renewable and Sustainable Energy Reviews, 19, 238-246.

Bolaji, B. O. (2006) "Flow design and collector performance of a natural circulation solar water heater" Journal of Engineering and Applied Sciences. 1(1), 7-13.

El-Shatoury, R. S. (2005) "Effects of the plants density and nitrogenous fertilizer on growth characters of summer squash" Master of Science, Horticulture department, Faculty of Agriculture, Suez Canal University, Egypt.

Ghosal, M. K. and Tiwari, G. N. (2006) "Modeling and parametric studies for thermal performance of an earth-to-air heat exchanger integrated with a greenhouse" Energy Conversion and Management August, 47 (13-14): 1779-1798.

Ghosal, M. K.; Tiwari, G. N.; Das, D. K. and Pandey, K. P. (2005) "Modeling and comparative thermal performance of ground air collector and earth air heat exchanger for heating of greenhouse" Energy and Buildings, 37, 613-621.

Guihua, Li.; Runsheng, T. and Hao, Z. (2012) "Optical Performance of Horizontal Single Axis tracked Solar Panels" International Conference on Future Energy, Environment and materials, 16, 1744-1752.

Hassanien, R.H.E.; Li, M. and Tang, Y., (2018) "The evacuated tube solar collector assisted heat pump for heating greenhouses". Energy Build, 169, 305-318.

Imre, L. (2020). "Solar drying" CRC Press 373-451.

Khan, M. T. A.; Tanzil, S. M. S.; Rahman, R. and Alam, S. M. S. (2010) "Design and Construction of an Automatic Solar Tracking System". 6th International Conference on Electrical and Computer Engineering, 18 – 20 December, Dhaka, Bangladesh.

Kishk, S. S. and Abu-Zeid, M. A. (2019) "Experimental Evaluation of Two Serpentine Flat Plate Solar Water Heating Systems". Misr Journal of Agricultural Engineering, 36(2), 629-642.

Kishk, S.S. (2014) " Earth Air Heat Exchanger System for Cooling and Heating Greenhouses During Summer and Winter Seasons" Horticultural Produces. Ph.D. Dissertation. Agric. Eng. Dept. Faculty of Agricultuer, Suez Canal University, Egypt

Kumar, K. S.; Tiwari, K. N. and Madan, K. (2009) "Design and technology for greenhouse cooling in tropical and subtropical regions: A review" Energy and Buildings, 41, 1269-1275.

Kurtbas, I. and Turgut, E. (2006) "Experimental Investigation of Solar Air Heater with Free and Fixed Fins: Efficiency and Exergy Loss". International Journal of Science & Technology, 1 (1) 75 - 82.

Li, H.; Yu. Y.; Niu, F.; Shafik, M. and Chen, B. (2014) "Performance of a coupled cooling system with earth-to-air heat exchanger and solar chimney" Renewable Energy, 62, 468-477.

Milun, S.; Klic, T. and Bego, O. (2005) "Measurement of soil thermal properties by spherical probe" IEEE transactions on instrumentation and measurement, 54 (3).

Nayak, S. and Tiwari, G. N. (2010) "Energy metrics of photovoltaic/thermal and earth air heat exchanger integrated greenhouse for different climatic conditions of India" Applied Energy, 87, 2984-2993.

Nelson, V. P. (2006) "Greenhouse operation and management" Fifth Edition, A Reston Book, Prentice-Hall, Inc, Englewood cliffs, New Jersey, USA, 598pp.

Ozgener, O. and Hepbasli, A. (2007) "A parametrical study on the energetic and exergetic assessment of a solar-assisted vertical ground-source heat pump system used for heating a greenhouse" Building and Environment, 42, 11–24.

Shukla, A.; Tiwari, G. N. and Sodha, M. S. (2006) "Thermal modeling for greenhouse heating by using thermal curtain and an earth–air heat exchanger" Building and Environment, 41, 843-850.

Tiwari, G. N. (2003) "Greenhouse technology for controlled environment" India: Narosa Publishing House.

Tiwari, G. N.; Akhtar, M. A.; Shukla, A. and Khan, E. M. (2006) "Annual thermal performance of greenhouse with an earth–air heat exchanger: An experimental validation" Renewable Energy, 31, 2432-2446.

Vandecasteele, B.; Blindeman, L.; Amery, F.; Pieters, C.; Ommeslag, S.; Van Loo, K.; De Tender, C. and Debode, J. C. P. (2020). "Grow-Store-Steam-Re-peat: Reuse of spent growing media for circular cultivation of Chrysanthemum" 276, 124128.

Watane, N. D. and Dafde, R. A. (2013) "Automatic solar tracker system". International Journal of Scientific & Engineering Research, 4 (6), 93-100.

Xu, W.; Song, W. and Ma, C. (2020) "Performance of a water-circulating solar heat collection and release system for greenhouse heating using an indoor collector constructed of hollow polycarbonate sheets". Journal of Cleaner Production 253, 119918.

Yano, A., Cossu, M. J. R., & Reviews, S. E. (2019) "Energy sustainable greenhouse crop cultivation using photovoltaic technologies". 109, 116-137.

Zhao, Y.; Li, R.; Ji, C.; Huan, C.; Zhang, B. and liu, L. (2019) "Parametric study and design of an earth-air heat exchanger using model experiment for memorial heating and cooling". Applied Thermal Engineering 148, 838-845.

تقليل الانحراف الحراري داخل البيوت المحمية باستخدام التسخين الشمسي وأنابيب الهواء التحت أرضية

سامح سعيد كشك[١]، إسلام حسن الشيخ[٢] و يحيى عجيز [٣]

[١] أستاذ مساعد الهندسة الزراعية - كلية الزراعة - جامعة قناة السويس - مصر.

[٢] أستاذ الهندسة الزراعية - كلية الزراعة - جامعة قناة السويس - مصر.

[٣] معيد بقسم الهندسة الزراعية - كلية الزراعة - جامعة قناة السويس - مصر.

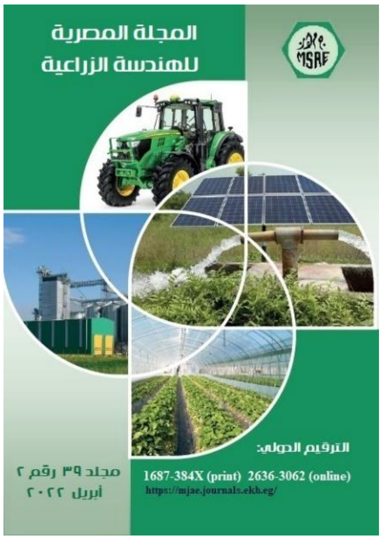

© **المجلة المصرية للهندسة الزراعية**

الكلمات المفتاحية:

الصوب الزراعية؛ مبادلات الهواء التحت أرضية؛ التسخين الشمسي؛ التعقب الشمسي .

الملخص العربي

تهدف الدراسة إلى استخدام التسخين الشمسي ومبادل الهواء التحت أرضى لتوفير الظروف المثلى لنمو محصول الخيار داخل البيوت المحمية. استخدمت للتجربة ثلاث صوب من البلاستيك على شكل الجمالون المتناظر الانحدار بمساحة ارضية ٢٤ م٢ بمزرعة كلية الزراعة جامعه قناة السويس خلال شتاء ٢٠٢٠. الصوب مصنوعة من مواسير المياه المجلفنة بقطر واحد بوصة ومغطاه بطبقة مزدوجة من البولي إيثيلين بسمك ١٥٠ ميكرون أيضاً تم توجيه الصوب الثلاثة باتجاه شرق غرب. الصوبة الاولى يتم تسخينها بمجمع مياه شمسي مزود بنظام تعقب شمسي. الصوبة الثانية متصلة بنظام مبادل الهواء التحت أرضى أما الصوبة الثالثة تستخدم كصوبة مقارنة. نظام التسخين الشمسي مكون من أربعة أجزاء (أ) نظام تعقب شمسي (ب) مجمع مياه شمسي مسطح (ج) خزان معزول من البلاستيك سعة ٥٠٠ لتر (د) مبادل حراري مصنوع من مواسير الألومنيوم. نظام مبادل الهواء التحت أرضي تم تصميمه على عمق ٣ م بطول ٢٦ م وقطر ٦ بوصة. وقد توصلت الدراسة إلي:-

١. درجة حرارة ثبات التربة وجدت على عمق ٣ متر بمقدار٢١,٧ م° وتظل ثابتة عند وحول هذه القيمة.
٢. كفاءة نظام مبادل الهواء التحت أرضي تتناسب عكسياً مع درجة حرارة دخول وخروج الهواء. المتوسط الكلى للكفاءة الحرارية لنظام مبادل الهواء التحت أرضى ٦٥ % خلال فترة التدفئة.
٣. الكفاءة الحرارية الكلية لمجمع المياه الشمسي وجدت ٥٩,٦ %
٤. المتوسط الليلي لدرجات الحرارة للصوب الثلاثة والهواء الخارجي وجدت ١٢,٣ ، ١١,٦ ، ٩,٣ و٩,٤ م°
٥. كمية محصول الخيار للصوب (ج١ وج٢) أعلى إنتاجية بمقدار٩٧ و٦٦٪ مقارنة بصوبة الكنترول.